

# ISSUES CONCERNING THE INTERNATIONAL STANDARD OF ESD GROUND TEST FOR GEO SATELLITE SOLAR ARRAY

**Mengu Cho**

Kyushu Institute of Technology  
1-1 Sensui Kitakyushu, Japan 804-855  
Phone: +81-93-884-3228  
Fax: +81-93-884-3228  
E-mail: [cho@ele.kyutech.ac.jp](mailto:cho@ele.kyutech.ac.jp)

**Yoshio Shikata**

**Satoshi Hosoda**

**Kazuhiro Toyoda**

**Emanuel Amorim**

Kyushu Institute of Technology

**Tateo Goka**

Japan Aerospace Exploration Agency

**Leon Levy**

**Rene Reulet**

Office National d'Etudes et de Recherches Aerospatiales

**Denis Payan**

Centre National d'Etudes Spatiales

## **Abstract**

As the power level of Geostationary satellites increases, there is more demand of careful ground test on solar array insulation strength. International atmosphere surrounding commercial telecommunication satellites calls for common international standard on test conditions. The issues regarding test environment, test circuit, test duration and external capacitance are reviewed. Results of experiment on the influence of external capacitance on secondary arc formation are presented.

## **Introduction**

Since the last decade, the power level of a geostationary satellite has increased dramatically to nearly 10 kW or even higher. To manage the large amount of power efficiently, nowadays

many commercial telecommunication satellites employ solar array that generates the electricity at 100V.

As the voltage of solar array increases to 100V, arcing during substorm has been recognized as serious hazard that sometimes threatens the stable supply of the solar array power. In Geosynchronous Orbit (GEO), when a satellite receives the sunlight, its charging is dominated by photoelectrons. As long as the satellite surface is well illuminated under the quiet condition, photoelectrons keep the satellite potential within a few electron volts from the plasma potential. Insulator surface such as coverglass has similar potential. When a satellite encounters substorm, the current due to high-energy electrons increases and sometimes exceeds the current due to photoelectrons. Then the potentials of the satellite body and the insulator surface can become negative. Due to the difference of the secondary electron emission coefficients, the insulator potential may drop slower than the satellite body. During that process, the coverglass potential can be more positive than the nearby conductor, e.g. interconnector. This situation is called "inverted potential gradient". In the present paper we call the potential difference between the coverglass and the satellite body *differential voltage*. The differential voltage,  $\Delta V$ , is defined in the following equation;

$$\Delta V = \phi_{cg} - \phi_{sat} \quad (1)$$

where the satellite potential is equal to the interconnector potential at the negative end of the solar array circuit. As the differential voltage builds up between coverglass and interconnector, an arc may occur. It is well known that an arc occurs once the differential voltage reaches 100 or 200V in LEO plasma condition<sup>(1,2)</sup>. Cho et al<sup>(3)</sup> found that an arc may occur with the differential voltage of as low as 400V under simulated GEO plasma conditions during a ground experiment.

In Fig.1 we illustrate the definitions of arc phenomena discussed in this paper. If an arc occurs as a single pulse, we call it a *trigger arc*, a *primary electrostatic discharge* (ESD) or a *primary arc*. For the rest of present paper, we call it primary arc. There are two current paths of a primary arc. One is current 1 in Fig.1 that flows between spacecraft and the ambient plasma, where a capacitance of satellite body, typically of the order of 100pF provides energy. The other is current 2 in Fig.1 that flows between the arc point and insulator surface on spacecraft, where a capacitance of coverglass, at maximum more than 10 $\mu$ F, mostly provides energy.

If an arc occurs at a gap of two solar array strings or near defect of the insulator layer between cells and conductive substrate, there is a risk of one primary arc growing to a catastrophic arc receiving energy from the array itself. The risk has increased recently as the power level of solar array has increased. When an arc occurs, the arc plasma may short-circuit two points on solar array panel with different potentials, that is called *secondary arc*. The secondary arc has three stages as shown in Fig.2. The first stage is *non-sustained arc* that

continues only while the primary arc current flows. The second stage is *non-permanent sustained arc* that has a current pulse longer than that of the primary arc. The third stage is *permanent sustained arc* where the current is maintained by the solar array string circuit and keeps flowing until the solar array string circuit is disconnected. The sustained arc gives excessive heat to underlying insulation substrate. Thermal breakdown of the insulation substrate leads to permanent short-circuit of solar array strings. Several satellites<sup>(4,5)</sup> lost a part of solar array output power due to the sustained arc. The risk of sustained arc increases as output voltage of solar array increases, because the potential difference between two points short-circuited by the arc plasma becomes higher.

As size and price of GEO satellites become larger, there is more demand for careful ground test before launch. Ground tests are being carried out to confirm whether a given design of solar array can withstand the sustained arc. In Fig.2 we schematically illustrate experimental layout of a typical ground test. We place a solar array coupon inside a vacuum chamber. The coverglass surface is charged more positively than the solar cells either by an energetic electron beam or by positive ions. One string of solar cells is biased to a positive potential with respect to the conductive substrate, simulating the positive end of solar array. Another string is grounded (or sometimes connected through a resistance) to the conductive substrate, simulating the negative end of solar array. The positive potential given to the first string,  $V_{gap}$ , should be equivalent to solar array output voltage,  $V_{out}$ . The floating power supply simulates the solar array string circuit. The power supply should act as a constant voltage source before an arc and should act as a constant current source once the arc plasma short-circuits the strings or the string and the substrate. The maximum current provided by the power supply should be equivalent to the solar array short-circuit current,  $I_{sc}$ .

When we carry out an ESD test of solar array, proper test conditions that simulate the conditions in orbit are necessary. Inadequate testing conditions lead to unexpected failure in space. Increasing the level of harshness beyond a reasonable limit is not always a good solution. There is not yet any standard on how we carry out the ESD test on solar array. There are currently four major issues regarding the ESD test method.

- (1) How do we charge the coverglass to produce the inverted potential gradient?
- (2) What type of power supply do we use to simulate the solar array string circuit?
- (3) How long do we carry out the test?
- (4) How do we implement the role of capacitance associated with coverglass of solar array panel that cannot be accommodated into the vacuum chamber?

As manufacturers, subcontractors, launchers, users and insurers of GEO telecommunication satellites have become international, there is more need of international standard on the ESD test

method. The purpose of the present paper is to describe the four issues in detail to stimulate the discussion to establish the common standard. There are many aspects in ESD test. In this paper we focus on the test that investigates the insulation strength of a given solar array design against the sustained arc phenomena.

### **Test Environment**

Because a secondary arc occurs only when a primary arc occurs on a solar array coupon, to investigate the insulation strength against the sustained arc, we want primary arcs as many as possible. Table 1 lists the summary of three typical environment where ESD tests are carried out. The electron beam environment uses an energetic electron beam whose energy is typically of the order of keV. The electron beam charges the coverglass surface more positive than the solar array circuit by inducing secondary electron emission. Typical background pressure is of the order of  $10^{-6}$  Torr or less. The plasma environment uses plasma as dense as Low Earth Orbit (LEO), such as  $10^{10}\sim 10^{12}\text{m}^{-3}$  to charge the coverglass surface. The plasma is usually produced via a diffusion type glow discharge device and its temperature is of the order of 1eV. The background pressure during the test is of the order of  $10^{-5}$  Torr or more. The ion beam environment uses an ion beam whose energy is 1keV or less. The background pressure is similar to the plasma environment because the ions are extracted from the glow discharge device.

Usually the plasma environment gives the highest rate of primary arcs (arc rate), because recharging of coverglass via the dense plasma is fast and the background pressure is high. Figure 2 shows a picture of solar array coupon used for the ESD test of ETS8 solar array<sup>(3,6)</sup>. Two identical coupons were tested in the same vacuum chamber for different environments, the electron beam environment and the plasma environment. In the electron beam environment where the electron current density was between  $30\mu\text{A}/\text{m}^2$  and  $3\text{mA}/\text{m}^2$  the arc rate was only 10 to 20 arcs per hour. On the other hand, in the plasma environment, the arc rate was more than 10 arcs per minute. Thermal ion current density in the plasma environment is of the order of  $10\mu\text{A}/\text{m}^2$ . Although this number is comparable to the electron beam current density, the solar array coverglass can collect ions crossing the sheath boundary surrounding the solar array coupon with much larger surface area than the coupon itself. Therefore, the actual current density charging the coverglass is much higher than the simple one-dimensional thermal current density.

There is no doubt that the electron beam environment provides the best simulation of inverted potential gradient in GEO that is caused by energetic electrons generated by substorm. Because we want the arc rate as high as possible, however, we are tempted to use the plasma environment to test a solar array coupon against sustained arc. Because the sustained arc phenomena is usually short-circuit of two points that are separated only by one millimeter or less, the phenomena may not depend on the nature of background conditions as long as a primary arc occurs. To make sure that the ESD tests carried out under the plasma or ion beam environments

are representative of GEO conditions, the effects of background plasma density and neutral density on the sustained arc formation must be studied. The best way is to confirm the sustained arc thresholds for string voltage, string current and cell gap distance are independent of the background parameters via experiments using the same test coupons in different environments. At least we should verify that the results in the plasma environment are scalable to the results in the electron beam environment.

### **Test circuit**

To study sustained arc phenomena, we have at least two DC power supplies. One is a power supply to bias the solar array coupon negatively with respect to the chamber ground, which is shown as  $V_b$  in Fig.3. DC negative voltage given by this power supply simulates the satellite potential with respect to the space plasma when a satellite is severely charged by energetic electrons. We can charge the solar array coupon negatively by an electron beam alone. But, it is very difficult to control the coupon potential. Stable DC output voltage is required for the first power supply but not much capacity of current.

Another power supply simulates the solar array string output power that provides energy to the arc plasma once a secondary arc occurs, which is shown as  $I_{sc}$  in Fig.3. We call this power supply *string power supply* in this paper. The requirement for the string power supply was described by Payan *et al.*<sup>(7)</sup>. Basically the string power supply must behave in a very similar way to the real solar array circuit. Two strings on the test coupon are insulated before the primary arc inception. Therefore the power supply should provide a constant voltage,  $V_{gap}$ , between the two strings. Once the secondary arc plasma short-circuits the two strings, the voltage collapses and a constant current is provided. After the secondary arc inception, the second power supply must act as a constant current source that can provide the solar array short circuit current at maximum. Figure 5 shows a schematic picture of string power supply<sup>(7)</sup>. Three diodes ensure that a voltage determined by  $V_{gap}=I_s R_L$  is kept before secondary arc inception and all of  $I_s$  can flow between the strings once the string gap is short-circuited by plasma. The DC power supply  $V_L$  keeps the voltage across the load  $R_L$  that simulates the satellite load even after the secondary arc, which is true for a real satellite as the bus voltage is maintained by other strings.

Transient current that flows at the transition from a primary arc to a secondary arc heavily affects the outcome of the secondary arc. Figure 6 schematically shows a waveform of secondary arc current. There is an overshoot at the beginning that is caused by capacitances parallel to the string gap. The current also shows oscillation after the initial overshoot that is caused by inductance associated with the string circuit.

There are three types of capacitance, capacitance of polyimide insulator and adhesive

between cells and conductive substrate, capacitance of cell PN junction and output capacitance of power supply. The first two capacitances exist in a real satellite, but not the third one. The combination of the first two capacitances is represented by  $C_1$  and  $C_2$  in Fig.5. These values of capacitance can be calculated regarding the solar array circuit as a distributed parameter circuit. The output capacitance of power supply varies depending on its type. When we use a conventional DC power supply that acts either as a constant voltage source or a constant current source, the output capacitance is even larger than  $100\mu\text{F}$ . Therefore if we use a conventional DC power supply to give  $V_{gap}$ , the overshoot is very large and it takes a relatively long time, sometimes even longer than  $1\text{ms}$ , to reach the steady state value,  $I_s$ . The energy supplied by the output capacitance does not exist in reality. Therefore, if we use a conventional power supply, we give a significant amount of overstress to the gap. It is recommended that we use a solar array simulator that has a small output capacitance of  $100\text{nF}$  or less. Also, if we operate the solar array simulator in a constant current mode before the arc inception, the effect of output capacitance becomes even smaller.

The oscillation caused by inductance may lower the probability of secondary arc occurrence. If there is too much inductance, the secondary arc current becomes negative crossing zero. As it crosses zero, it might be terminated. Therefore, cable length must be as short as possible to avoid the unnecessary oscillation. In real solar array circuit, however, there is also inductance. We need a good estimate on the value of inductance to make the experimental circuit as realistic as possible.

### **Test duration**

Inverted potential gradient that is responsible for primary arcs occurs only occasionally in orbit. Another paper presented in this conference<sup>(8)</sup> describes statistical analysis of GEO plasma environment and estimate on total number of primary arcs. For a given set of satellite geometry and surface material property, potentials of satellite body and insulator surface are determined by the combination of solar incident angle and plasma parameters such as electron temperature, electron density, ion temperature and ion density<sup>(2,8,9)</sup>. Once these parameters are known, it is possible to calculate the potentials for each case within certain accuracy using commercial software such as NASCAP/GEO<sup>(10)</sup>.

From the statistical analysis, we can calculate expected duration of any combination of the plasma parameters. From the numerical simulation we can calculate the differential voltage,  $\Delta V$ , for each case of the plasma parameters. If we know the threshold of primary arc inception in terms of differential voltage, we can calculate how long a satellite goes through the inverted potential gradient exceeding the threshold by combining the statistical analysis and the numerical simulation. If the numerical simulation code can properly calculate the temporal profile of the

potentials, we can deduce the number of primary arc by dividing the duration exceeding the threshold by the time for  $\Delta V$  to reach the threshold.

From the total number of expected arcs in orbit, we can set a number of primary arcs that a test solar array coupon must endure to prove that it has sufficient insulation strength against the sustained arc. The insulation strength may degrade over time in orbit as solar array surface is exposed to ultra-violet (UV) ray, radiation or thermal cycles. The effect of these environmental factors on the insulation strength is still unknown. If the effect is negligible and test results in the plasma environment discussed in Sec.II are scalable to the GEO environment, we can finish the ESD test quickly by using the plasma environment.

### **External Capacitance**

As shown in Fig.1, capacitance of satellite body with respect to space,  $C_{sat}$ , and capacitance across coverglass,  $C_{cg}$ , provide energy to a primary arc. The coverglass capacitance has been a subject of controversy. As a primary arc occurs, it quickly discharges the satellite capacitance via the current path 1 in Fig.1. Then the satellite body potential that is very negative before the arc inception jumps to near zero. The coverglass potential then becomes positive by  $\Delta V$  with respect to the plasma. If the satellite were in LEO-like dense plasma, the positive coverglass surface would attract electrons and a large amount of electrostatic energy could be provided to the primary arc plasma as the coverglass charge is neutralized<sup>(10,11,12)</sup>. In tenuous plasma like GEO, the conductivity of ambient plasma is so low that the arc plasma itself has to neutralize the coverglass charge. Therefore, there is no guarantee the mechanisms of coverglass charge neutralization in LEO environment and GEO environment are same. Leung *et al.*<sup>(13)</sup> carried out an experiment using a large solar array coupon and showed that the plasma extends itself as far as 0.7m with a speed of  $9 \times 10^3$  m/s in GEO-like environment.

Because we cannot place the whole solar array panel in a vacuum chamber, the majority of the coverglass capacitance is usually simulated by a capacitor connected to the external circuit,  $C_{ext}$ , shown in Fig.3. The external capacitance represents both  $C_{sat}$  and  $C_{cg}$ , but the satellite capacitance is so small that even the capacitance of circuit cable, typically 100pF/m, might exceed the value. Therefore, the external capacitance  $C_{ext}$  is determined by how we implement the role of coverglass capacitance that is missing from a test coupon. Typical  $7cm \times 3.5cm \times 100\mu m$  size coverglass has about 700pF each. For a 10kW-class satellite the total capacitance coverglass may exceed 10 $\mu$ F.

The amount of external capacitor currently employed differs among research institutions, ranging from 100pF ( i.e.  $C_{sat}$  only) to 1 $\mu$ F. Because the electrostatic energy is given by

$\frac{1}{2}C_{ext}V_b^2$ , not  $\frac{1}{2}C_{cg}\Delta V^2$  and  $|V_b| \gg \Delta V$ , employing  $1\mu\text{F}$  is equivalent to employing  $C_{cg}$  of entire solar array paddles. The effect of external capacitance on a primary arc is significant. The larger the external capacitance, the higher and longer current flows in the primary arc. In this paper we call the primary arc current provided by  $C_{ext}$  *blow-off current*. Solar cells are sometimes damaged and suffer contamination when too much energy is injected from the external capacitance<sup>(14,15)</sup>.

How much of charge from coverglass flow as the blow-off current and how fast primary arc plasma becomes a secondary arc could be the different problems, though. Once a primary arc becomes a secondary arc, the solar array strings provide energy to the arc plasma and the coverglass capacitance might affect little. If we focus only on the transition from the primary arc to the secondary arc, we might not need to consider the entire solar array paddle as the source of capacitance. We have carried out an experiment to study the properties of primary arc and secondary arc plasmas while varying the value of  $C_{ext}$ . The specific purpose of the experiment is to find the value of external capacitance beyond that the transition process from a primary arc to a secondary arc differs little. If we find such an upper bound, we have the appropriate value as the coverglass capacitance for the ESD test on the secondary arc. If the value is reasonably small, we can represent the coverglass capacitance only by the solar array coupon panel and avoid the controversial external capacitance. Even if the value is so big that we need the external capacitance, we can limit the value of external capacitance and avoid unnecessary overestimate on the damage caused by primary arc.

In Fig.7 we show the experimental circuit layout. Figure 8 shows photograph of test coupons used for the experiment. The experimental circuit and test coupons are kept as similar as possible to the earlier works carried out at ONERA<sup>(16)</sup>. The present experiment is carried out in a vacuum chamber at KIT. The purpose of using the same setup is to share the experimental results carried out at two different institutions by keeping consistency. One of the authors (E. Amorim) stayed at KIT for four months to participate in the initial phase of experiment. The string power supply in the experimental circuit is the same as the one shown in Fig.5. Once a primary arc occurs, the coupon potential rises and the detector sends a signal to the delay pulse generator. After a preset time delay, the pulse generator sends a gate signal to the spectrometer (Hamamatsu Photonix C8808) that is equipped with an image intensifier. The gate width for the present experiment is kept to  $1\mu\text{s}$ . By varying the time delay, we can study the plasma properties at the moment of transition from a primary arc to a secondary arc. We also use the quadruple mass spectrometer to identify species of gas ejected at arc inception. We irradiate the test coupon biased to  $-5\text{kV}$  by an electron beam of  $5.2\text{kV}$  energy. The test coupon is made of two plates of copper glued on insulating substrate. The copper plates simulate solar cells. They are separated by  $0.9\text{mm}$ . In order to simulate coverglass, PET film and SSM Teflon film are placed on top of



the copper plate. Because we want a primary arc occur at the focus of spectrometer, we put scars at one side of copper plate. Only a part of metallic edge of copper plate is exposed and the other part is insulated by narrow polyimide film. The video camera records flashes associated with primary arcs. We identify the arc position by identifying the positions of primary arcs and disregard the spectrometer data if the primary arc does not occur within the focus of spectrometer.

Table 2 summarizes the experimental results. We have tested three types of coupons varying their sizes. We judged whether a given arc current was a secondary arc current or not based on the three criteria; (1) the current exceeded 1.3A (2) the current pulse width was longer than 10 $\mu$ s (3) the current continued even after the end of blow-off current pulse. The number of secondary arcs was much less than the number of primary arcs. It should be noted that secondary arcs occurred even for zero external capacitance,  $C_{ext}=0$ . In Fig.9 we show current waveforms of secondary arcs for  $C_{ext}=0$ . For this particular case, the secondary arc current continued up to 90 $\mu$ s. There were several other cases of secondary arc though they didn't last as long as the case shown in Fig.9. In Fig.10 we show a current waveform of secondary arcs for  $C_{ext}=100nF$ . For this case the secondary arc current continued 12 $\mu$ s. Figure 11 plots duration of secondary arcs for different values of  $C_{ext}$ . In the figure the results of sample 2 and 3 are combined. In order to increase the number of data points, we have added the data taken in a different series of experiment, though the experimental setting was the same, to the data listed in Table.2. There seems no dependence of the secondary arc duration on the value of external capacitance.

Figure 12 shows a typical spectrum observed for the sample No.2 with  $C_{ext}=12.5nF$ . At this time, only the blow-off current was flowing and the amplitude was 3.6A. We have identified strong lines of copper (324.7nm and 327.4nm), C<sub>2</sub> swan band and hydrogen (656.3nm). Copper atoms come from the metallic electrode. Carbon molecules probably come from insulator near the electrode or adsorbed molecules. Hydrogen atoms come from adsorbed water molecules. In Fig. 13 we plot a temporal profile of total pressure inside the vacuum chamber and partial pressure of copper measured by the mass spectrometer. The spikes in the total pressure indicate that primary arcs occur and adsorbed molecules are desorbed due to heat. Although very weak, we see spikes in the copper signal that result from vaporization due to the primary arcs.

Figure 14 shows the strongest lines in each spectrum taken at various values of blow-off current. The horizontal axis is the blow-off current that was flowing when the gate of spectrometer was open. The peak values of blow-off current are proportional to the external capacitance. When the blow-off current is higher than 8A, the copper line of 324.7nm dominates for most of the cases. The result is reasonable if the current at the arc spot is maintained by metallic vapor plasma evaporated from the electrode surface. The ratio of the two strong copper lines is relatively constant once the copper lines dominate over other lines. Figure 14 also shows

the ratio of the intensity of 327.4nm to the intensity of 324.7nm. They show little scatter for the blow-off current higher than 8A. If we derive electron temperature from this ratio assuming that the arc plasma is in local thermodynamic equilibrium, the temperature is about 1000K. This temperature is a little too low for typical vacuum arc plasma. These two lines originate from two energy states separated only by 0.03eV. Therefore, it is very difficult to derive accurate temperature with the resolution of the spectrometer used in the experiment ( $\pm 1.5\text{nm}$ ). Nevertheless, the fact that the dominant spectrum lines and their ratio stay relatively same once the blow-off current exceeds a certain value, 8A, suggests that there is an upper limit on plasma property such as temperature even if we increase the blow-off current by increasing the external capacitance,  $C_{ext}$ . To find the upper limit on the plasma property, especially electron temperature because arc plasma conductivity depends on the temperature not on the density, we need either finer resolution of the optical spectrum or multiple sets of lines used for the temperature derivation.

The present experimental results favor the use of external capacitance,  $C_{ext}$ , as small as satellite capacitance,  $C_{sat}$ , only. Secondary arc occurs even for  $C_{ext}=0$  and the spectrum differs little beyond 8A of the blow-off current. The experimental results presented in this paper are still preliminary, however. We need more detailed picture of how the primary arc plasma becomes a secondary arc by following the temporal variation of arc plasma properties. The final answer to the problem of the external capacitance will be obtained only after we know coupling mechanism of coverglass charge and primary arc current. To do so, we need to study arc plasma expansion with a large solar array coupon such as the one carried out by Leung *et al.*<sup>(13)</sup> in tenuous GEO-like plasma. The results will be used to determine the external capacitance for the test purposes other than insulation strength against sustained arc, such as contamination or power degradation due to repeated primary arcs<sup>(14)</sup>.

## **Conclusion**

In this paper we have discussed the state of our knowledge regarding the four issues concerning conditions of ESD test of GEO satellite solar arrays. The followings are the conclusions and proposed research topics necessary to improve the credibility of test results.

- (1) Because the plasma environment gives the highest arc rate, we want to use the plasma environment if possible. To do so, however, we have to make sure that the test results in the plasma environment is the same as or at least scalable to the test results in the electron beam environment.
- (2) The power supply that simulates the solar array string circuit should have output capacitance as small as possible. We need good estimates on capacitance and inductance of solar array string.

- (3) It is possible to estimate the number of primary arcs during operational lifetime of a given satellite. To test the insulation strength against sustained arc we should verify that no sustained arc occur even after the same number of arcs occurs on a solar array coupon. The effect of long duration degradation of insulation material due to exposure to space environment needs to be clarified.
- (4) Even if there is no external capacitance connected to a solar array coupon, a primary arc can become a secondary arc. Beyond a certain value of arc current, the metallic vapor becomes the dominant species of arc plasma. These preliminary results suggest that, if the test purpose is only to know whether sustained arc occurs or not, the satellite capacitance and only a fraction of total coverglass capacitance are sufficient as the external capacitance. We need to study temporal variation of arc plasma properties to verify this finding.

Environment	Electron beam	Plasma	Ion beam
Energy of charged particles	$> 1 \text{ keV}$	$\sim 1 \text{ eV}$	$\leq 1 \text{ keV}$
Background pressure	$\leq 10^{-6} \text{ Torr}$	$\geq 10^{-5} \text{ Torr}$	$\geq 10^{-5} \text{ Torr}$
Primary arc rate	low	very high	high
Plasma density	low	high	

**Table 1: Comparison of three environments of ESD tests used to produce inverted potential gradient on a solar array coupon**

Sample number	$C_{\text{ext}}$ (nF)	number of primary arcs	number of secondary arcs
2	0	45	0
2	1.5	34	0
2	6.8	58	0
2	12.5	79	9
2	50	60	0
2	100	70	1
3	0	82	3
3	12.5	89	1
3	100	102	24

**Table 2: Number of secondary arcs observed for different values of  $C_{\text{ext}}$ .**

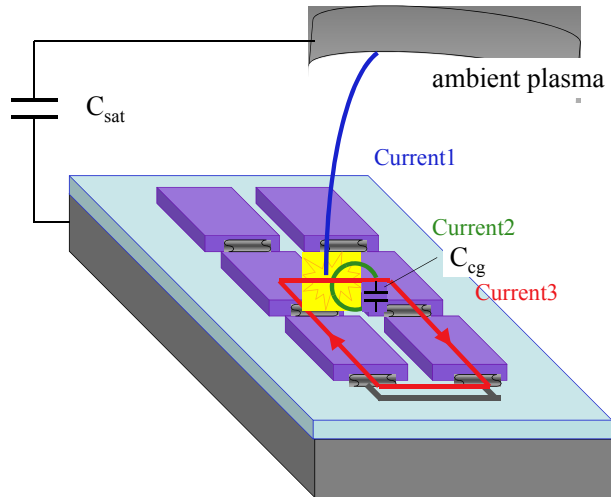


**Figure 1. Schematic illustration of arc current paths.**

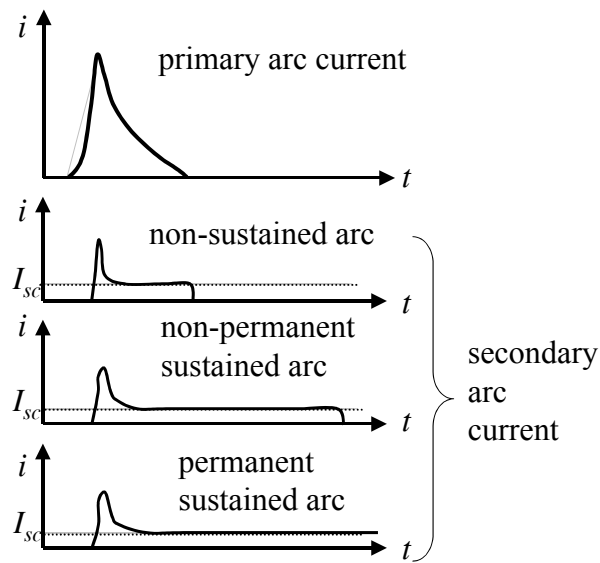


**Figure 2. Definitions of various stages of secondary arc current.**

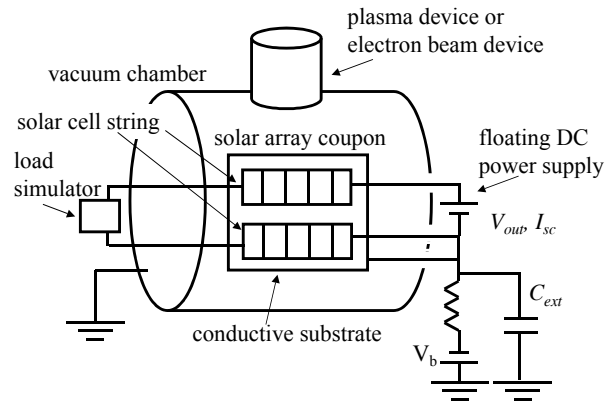


**Figure 3. Experimental layout of a typical ESD ground test with a solar array coupon.**

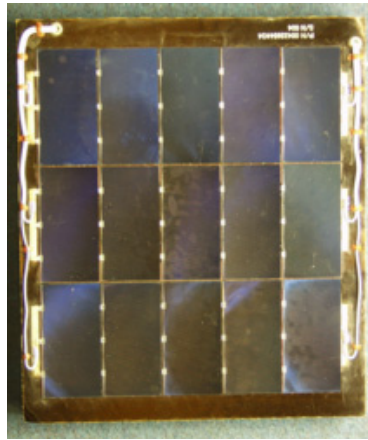


**Figure 4. Solar array coupon used for ETS8 solar array ESD test<sup>(2,6)</sup>**

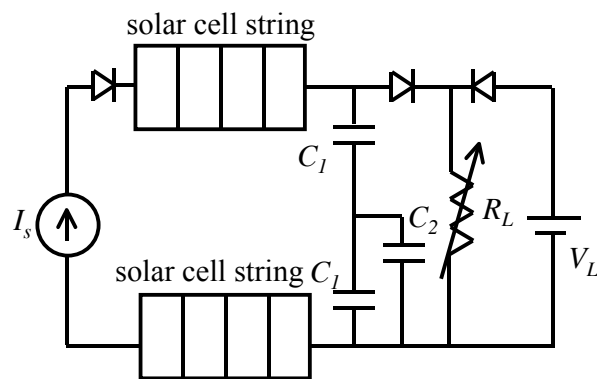


**Figure 5. Circuit layout of floating power supply described in Ref.7.**

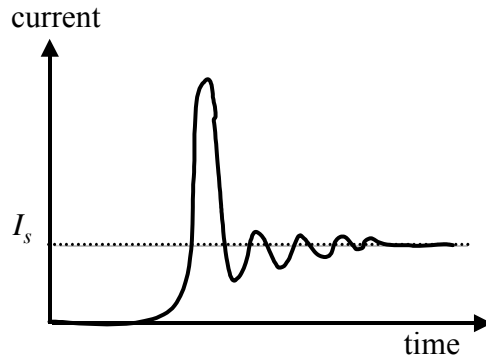


Figure 6. Schematic waveform of typical secondary arc current

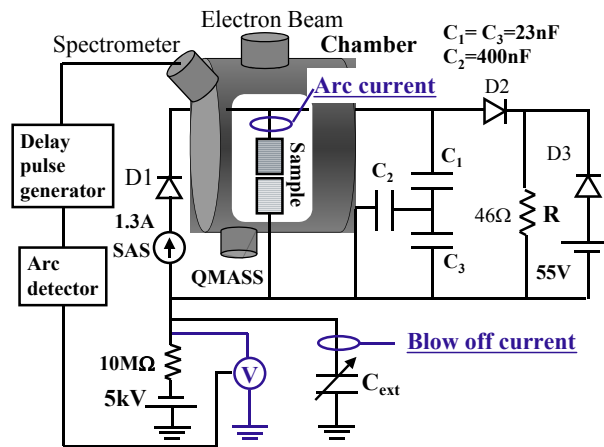


Figure 7. Schematic illustration of experimental circuit used to study the effects of external circuit

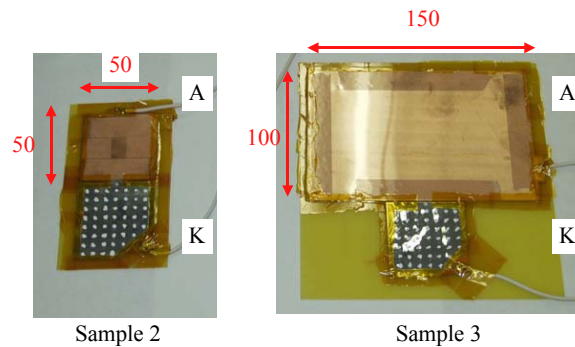


Figure 8. Photographs of test coupons used to study the effects of external circuit

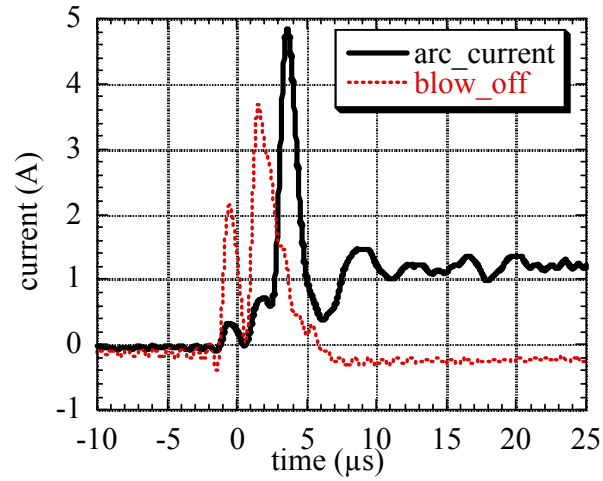


Figure 9. Example of waveforms of blow-off current and arc current with  $C_{ext}=0$

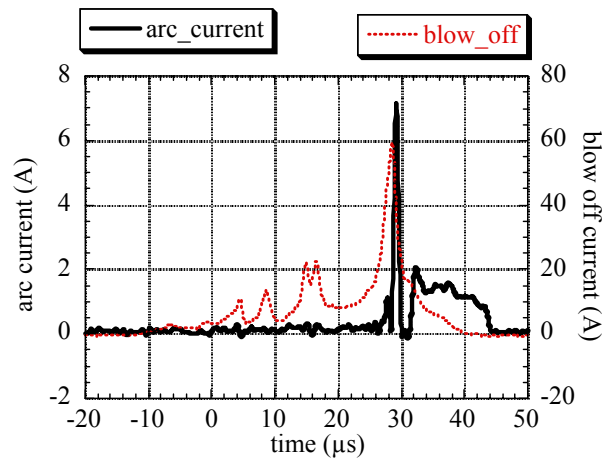
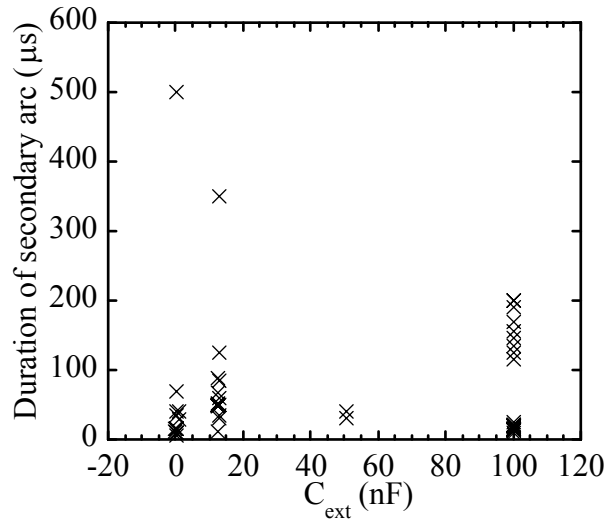
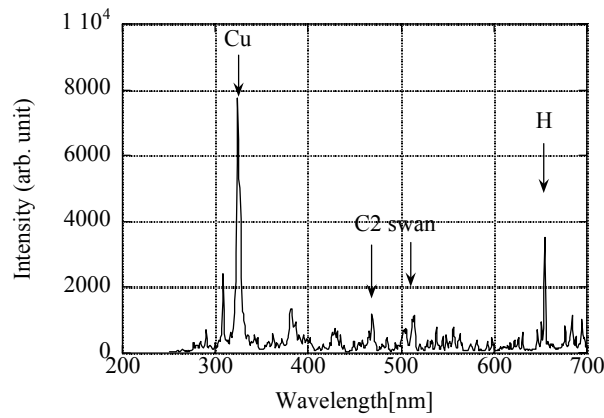


Figure 10. Example of waveforms of blow-off current and arc current with  $C_{ext}=100\text{nF}$



**Figure 11.** Duration of secondary arc for different values of external capacitance,  $C_{ext}$



**Figure 12.** Typical spectrum of arc plasma.

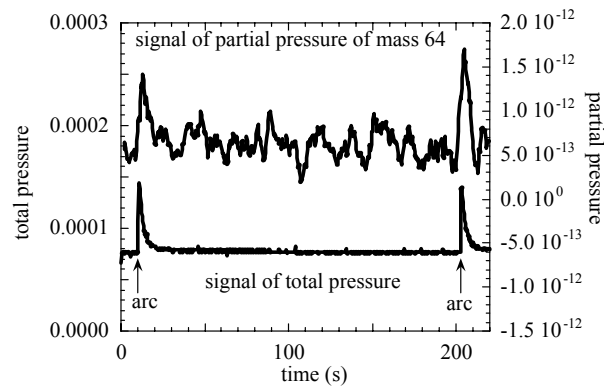


**Figure 13.** Signals of mass spectrometer during experiment



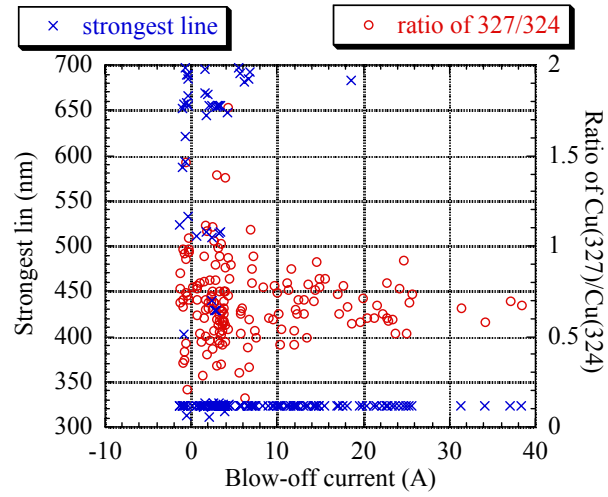


**Figure 14. Strongest lines for different values of blow-off current. The ratio of two copper lines at each blow-off current is also shown.**

## References

1. Ferguson, D. C., Snyder, D. B., Vayner, B. V., and Galofaro, J. T., "Array Arcing in Orbit from LEO to GEO", AIAA paper 98-1002, January 1999.
2. Hastings, D.E., Garrett, H., "Spacecraft-Environmental Interactions", Cambridge Univ. Press, New York, 1996.
3. Cho, M., Ramasamy, R., Matsumoto, M., Toyoda, K., Nozaki, Y., and Takahashi, M., "Laboratory Tests on 110V Solar Arrays in a Simulated Geosynchronous Orbit Environment", Journal of Spacecraft and Rocket, Vol.40, No.2, pp.211-220, 2003.
4. Katz, I., Davis, V.A; and Snyder, D.B, "Mechanism for Spacecraft Charging Initiated Destruction of Solar Arrays in GEO", AIAA paper 98-1002, January 1998.
5. Bogus, K., Claassens, C., and Lechte, H., "Investigations & conclusions of the ECS-Solar-Array in-orbit Power Anomalies", Proceedings of 18th IEEE Photovoltaic Space Conference, October-1985, pp.368-375.
6. Cho, M., Ramasamy, M., Toyoda, K., Nozaki, Y., and Takahashi, M., "Laboratory Tests on 110-Volt Solar Arrays in Ion Thruster Plasma Environment", Journal of Spacecraft and Rocket, Vol.40, No.2, pp.221-229, 2003.
7. Payan, D., Schwander, D., Catani, J.P., "Risks of low voltage arcs sustained by the photovoltaic power of a satellite solar array during an electrostatic discharge. Solar Array Dynamic Simulator", Proceedings of 7th Spacecraft Charging Technology Conference, April-2001, ESA.
8. Satoh, T., Nakamura, M., Kawakita, S., Takahashi, M., Nozaki, Y., Toyoda, K., Cho, M., "Development of Solar Array for a Wideband Internetworking Engineering Test and Demonstration Satellite: System Design", 8th Spacecraft Charging Technology Conference, October-2003, Huntsville, USA.
9. Lai, S. T., Delia-Rose, D.J., "Spacecraft Charging at Geosynchronous Altitudes: New Evidence of Existence of Critical Temperature", J. Spacecraft and Rockets, 38, (2001), pp.922-928.

10. Rubin, A. G., Katz, I., Mandell, M., Schnuelle, G., Seen, P., Parks, D., Cassidy, J. and Roche, J. "A Three-dimensional Spacecraft-charging computer code in Space Systems and their interactions with Earth's Space Environment", in Progress in Astronautics and Aeronautics, Vol.71, H. Garret, C. Pike, Ed., pp.318-336. 1980
11. Cho, M., Ramasamy, R., Hikita, M., Tanaka, K., Sasaki, S., "Plasma Response to Arcing in Ionospheric Plasma Environment: Laboratory Experiment", J. Spacecraft and Rockets, May-June, pp.392-399, 2002.
12. Vaughn, J.A., Carruth Jr., M.R., Katz, I., Mandell M.J. and Jongeward, G.A., "Electrical Breakdown Currents on Large Spacecraft in Low Earth Orbit", J. Spacecraft and Rockets, Vol.31, pp.54-59, 1994.
13. Leung, P., "Plasma Phenomena Associated with Solar Array Discharge and Their Role in Scaling Coupon Test Results to a Full Panel", AIAA Paper 2002-0628, 40th Aerospace Sciences Meeting, January 2002.
14. Toyoda, K., Matsumoto, T., Cho, M., Nozaki, Y., Takahashi, M., "Power Reduction of Solar Arrays due to Arcing under Simulated GEO Environment", AIAA 2003-0682, 41st Aerospace Science Meeting, 6-9 January, Reno, USA, 2003
15. Toyoda, K., Cho, M., Satoh, T., Nakamura, M., Kawakita, S., Takahashi, M., Nozaki, "Development of Solar Array for a Wideband InterNetworking Satellite : ESD Test", 8th Spacecraft Charging Technology Conference, October-2003, Huntsville, USA
16. Levy, L., Sarrail, D., Viel, V., Amorim, E., Serrot, G., Bogus, K., "Secondary arcs on solar arrays: occurrence, thresholds, characteristics and induced damage", Proceedings of 7th Spacecraft Charging Technology Conference, April-2001, ESA